High-Performance PET Fibers Via Liquid Isothermal Bath High-Speed Spinning: Fiber Properties and Structure Resulting from Threadline Modification and Posttreatment

JIUNN-YOW CHEN, PAUL A. TUCKER, JOHN A. CUCULO

Fiber and Polymer Science Program, College of Textiles, North Carolina State University, Raleigh, North Carolina 27695-8302

Received 16 September 1996; accepted 7 May 1997

ABSTRACT: Poly(ethylene terephthalate) fibers with improved mechanical properties and dimensional stability were spun via controlled threadline dynamics by a liquid isothermal bath (LIB) spinning process, followed by postdrawing and annealing. Control fibers were made by unperturbed spinning and posttreatment similar to a traditional spin–draw process. The two sets of as-spun fibers were spun at take-up speed in the range of 2000–5000 m/min. Fiber properties of the as-spun fibers and posttreated fibers of each process were compared. Two commercial tire cords, i.e., conventional tire cord and low shrinkage tire cord, were also included. Unlike unperturbed spinning, the LIB as-spun fibers show unique structural properties of high amorphous orientation, low crystallinity, high strength, and high initial modulus. Moreover, noncrystalline chains are further extended during posttreatment. The posttreated LIB fibers exhibit mechanical properties with tenacity higher than approximately 9 g/d, initial modulus higher than 120 g/d, and ultimate elongation less than approximately 10%. They also demonstrate superior dimensional stability with thermal shrinkage less than 6% and LASE-5 higher than 5 g/d. The overall properties are not obtainable by either the traditional spin–draw process or any modified process that produces low shrinkage tire cord. Unlike the case for unperturbed fibers, the mechanical properties of the posttreated LIB fibers demonstrate a strong/dependency on the birefringence of their respective as-spun fibers. There are at least three significant pieces of evidence that strongly indicate the existence of a third phase, referred to as the taut–tie noncrystalline phase (TTNC), in addition to the traditional two-phase model, i.e., crystalline and random amorphous phases. A unique feature involving a high fraction of taut–tie noncrystalline phase (TTNC %) in the LIB as-spun and the posttreated fibers is also found and which is, in fact, achieved neither by the traditional spin–draw nor the commercial tire cord processes. Further, different from the posttreated unperturbed fibers, the posttreated LIB fibers have an enhanced fraction of taut–tie noncrystalline chains with shorter length, which is believed to be one of the important factors leading to the superior mechanical properties and excellent dimensional stability achieved.
 J Appl Polym Sci **66:** 2441–2455, 1997

Key words: poly(ethylene terephthalate); high-performance fiber; threadline dynamics; high-speed spinning; taut–tie molecules; third phase

INTRODUCTION

Considerable research has been done in attempts to improve mechanical properties and dimensional stability of PET fibers. In a traditional spin–draw process, as-spun fibers are taken up at a relatively low speed, producing fibers in a random amorphous state with very low orientation and low crystallinity. The as-spun fibers are then subjected to postdrawing and annealing in several steps to gradually develop an oriented

Correspondence to: J. A. Cuculo.

Journal of Applied Polymer Science, Vol. 66, 2441–2455 (1997)
 CCC 0021-8995/97/13241-15

structure with appropriate high crystallinity. The traditional process produces fibers with high strength but relatively poor high temperature dimensional stability. This is a weak point and is undesirable in industrial end-use applications. In improving the thermal shrinkage of PET industrial yarn, a high-modulus low-shrinkage (HMLS) tire cord yarn was developed and commercialized. Although dimensional stability was improved, strength and initial modulus were unexpectedly not similarly improved.

When high-speed spinning, a one-step process (OSP), was introduced with promise of high productivity and cost reduction; the expected benefits, unfortunately, did not materialize. The high-speed spun fibers showed limited mechanical properties, with lower strength, lower initial modulus, and greater elongation than those of traditional spin–draw fibers.[1]

One of our main goals in high-speed spinning is learning how to control threadline dynamics via threadline modifications of both stress and temperature profiles by introduction of a tension enhancing liquid isothermal bath (LIB) in the spin line.[2–6] In this study, the LIB is placed near the structure development zone in the threadline with the expectation of increasing the amount of extended chains in as-spun fibers. In attempts to develop the full potential of these fibers, the oriented as-spun fibers are subjected to post drawing and annealing. The taut–tie noncrystalline chains are further rapidly developed and crystallized along the fiber axis. The structural properties of the LIB fibers are compared to the control, i.e., traditional spin–draw fibers, and two commercial yarns, i.e., conventional tire cord and low shrinkage tire cord fibers.

EXPERIMENTAL

Melt Spinning Process and Posttreatments

Poly(ethylene terephthalate) (PET) chips with intrinsic viscosity (IV) of 0.97 dL/g and viscosity molecular weight M_v of approximately 29,440 were used in this study. Before extrusion, PET chips were dried in a vacuum oven at 140°C for at least 16 hr. Spinning temperature was set at 298°C. A conventional spinneret with 0.6 mm diameter and $L/D = 3.0$ was used. A 5 cm heated sleeve set at 295°C was mounted beneath the spinneret to maintain uniform surface temperature. Unless otherwise specified, spinning/denier

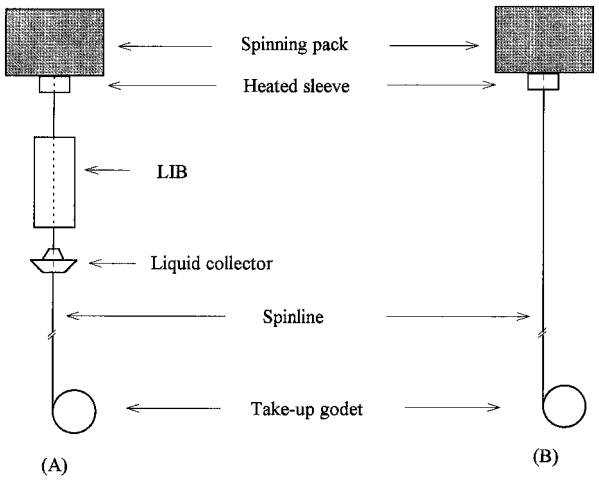

Figure 1 Schematic diagram of melt spinning via two different processes: (A) liquid isothermal bath (LIB) spinning process; and (B) unperturbed spinning process.

was set at 4.5. Figure 1 illustrates the two process setups employed in this study. One is the LIB process; the other, the unperturbed process. In the case of the LIB process, the liquid bath was positioned such that the bottom of the bath was 100 cm from the spinneret. The liquid medium, 1,2-propandiol, was heated at 175°C. Take-up speeds were set in the range of 2000–5000 m/min. The depth of liquid in the bath was kept at 45 cm for 2000–4000 m/min and 30 cm for 4000–5000 m/min take-up speed. At 5000 m/min speed, two other LIB depths of 20 and 25 cm were used. A liquid collector was placed below the LIB to recycle the heated liquid and to allow the threadline to fall vertically downward without any direction change. Downstream, the spinline was cooled by ambient air at 23°C and taken up by high-speed godet rolls. In the unperturbed process, the threadline was quenched only by ambient air without applying the LIB in the spinline.

Samples of as-spun fibers were then selected and subjected to a continuous posttreatment consisting of passing the fibers over two heaters between three rolls and then to a wind-up. The temperature of the first step, drawing, was set at 180°C, and the second step, annealing, at 220°C. The feed roll was controlled at a constant speed of 10 m/min. This speed was limited simply by the capability of the drawing equipment. The as-spun fibers were drawn mainly to a near-maximum draw ratio in the first step and only to a minimal draw ratio in the second step to retain threadline stress. A selected posttreated fiber was further

heat-set in a nitrogen-purged oven at 185°C for 10 min under constant length.

Characteristics of As-Spun and Posttreated Fibers

Birefringence

Birefringence was measured on a Nikon polarizing microscope with a Leitz tilting compensator. The average birefringence was based on five individual fiber samples.

Tensile Testing

An Instron tensile tester model 1122 was used to measure tenacity, ultimate elongation, initial modulus, and load at a specified elongation of 5% (LASE-5)[7] according to ASTM D3822-90. The single fiber sample was tested at a gauge length of 25.4 mm and a constant crosshead speed of 20 mm/min. An average from at least five individual tensile tests was obtained for each sample.

Differential Scanning Calorimetry

The thermal analyses were performed on a Perkin-Elmer Series 7 differential scanning calorimeter. Differential scanning calorimetry (DSC) curves were recorded during the first heating of approximately 2 mg fiber sample in the temperature range of 40 to 300°C with a heating rate of 20°C/min.

Boil-Off Shrinkage and Thermal Shrinkage

Boil-off shrinkage (BOS) was determined by immersing fiber samples in boiling water for 5 min in accordance to ASTM D2102-79. Thermal shrinkage was measured in a hot air oven at 177°C using ASTM D885 procedure as a general guide. The fiber length was measured under a pretension of 0.05 ± 0.01 g/d,[8] and the percent shrinkage was calculated using the following equation:

$$\text{Shrinkage}\ (\%) = \frac{l_0 - l}{l_0} \times 100 \qquad (1)$$

where l_0 is the initial fiber length, and l is the fiber length after treatment.

Density and Crystallinity

Density measurements were run in accordance with ASTM D1505-68. The density column contained sodium bromide solution (NaBr). The relative volume fraction crystallinity (X_v) was calculated as

$$X_v = \frac{\rho - \rho_a}{\rho_c - \rho_a} \qquad (2)$$

where ρ is the measured fiber density, ρ_a is the density of the amorphous phase, and ρ_c is the density of crystalline phase. The values of ρ_a and ρ_c are 1.335 and 1.455 g/cm^3, respectively.[9]

Radial Structure

A Jena interference microscope with a computer-aided interference microscope operating system[10] (IMOS) was employed to determine fiber radial birefringence. The measurement procedure is given in Lin et al.[10]

Wide-Angle X-Ray Scattering

The wide-angle X-ray scattering (WAXS) analysis of the PET fiber samples was performed on a Siemens Type F diffractometer equipped with a nickel-filtered CuK_α radiation (λ = 1.542 Å). The equatorial diffraction profile was fitted into three Pearson VII functions, as reported by Heuvel and Huisman,[11,12] with a correction of two Gaussian functional amorphous peaks at 17.5 and 23.5°, as documented by Murthy et al.[13] The peak in the meridional direction was $(\bar{1}05)$ at $2\theta = 43°$. Apparent crystal sizes were determined by the Scherrer equation.[14]

$$L_{hkl} = \lambda/(\beta \cos \theta) \qquad (3)$$

and the $(\bar{1}05)$ reflection was used to determine the crystalline orientation factor (f_c), calculated as

$$f_c = \frac{1}{2}(3\langle \cos^2 \phi_{c,z} \rangle - 1) \qquad (4)$$

A detailed description is in previous publication.[4] The amorphous orientation factor (f_a) is determined by applying the following equation:

$$f_a = \frac{\Delta n - \Delta n_c^0 f_c X_v}{\Delta n_a^0 (l - X_v)} \qquad (5)$$

where Δn is the fiber birefringence determined by a polarizing microscope with a tilting compensator, X_v is the volume fraction crystallinity measured from the density method, and Δn_c^0 and

Δn_a^0 are intrinsic birefringences of the crystalline and noncrystalline phase, respectively. The values of Δn_c^0 and Δn_a^0 are 0.22 and 0.275,[15] respectively.

Fraction of Taut–Tie Noncrystalline Phase

The fraction of taut–tie noncrystalline phase (TTNC %) is calculated on the basis of a parallel series three-phase model with the assumption that the modulus of the taut–tie noncrystalline phase is equal to that of the crystalline phase and calculated by the following equation[16]:

$$\text{TTNC } \% = \frac{V_a E(E_c - E_a) - E_a(E_c - E)}{V_a E_c(E_c - E_a) - E_a(E_c - E)} \quad (6)$$

where, $V_a = l - X_v$, and the X_v is from eq. (2); E is obtained initial modulus; E_c is crystal modulus (ca. 858 g/d);[17,18] and E_a is amorphous modulus (ca. 18 g/d),[17] calculated by using the values of ρ_c and ρ_a, respectively.

RESULTS AND DISCUSSION

Properties of As-Spun and Posttreated Fibers

The Effect of Take-Up Speed on As-Spun and Posttreated Fibers

Birefringence versus take-up speed of as-spun and posttreated fibers is shown in Figure 2. The unperturbed as-spun fibers have, as expected, low birefringence at approximately 0.07–0.10. After drawing to their near maximum draw ratios of 1.7 for the 3000 m/min take-up, and 1.5 for the 5000 m/min take-up spun fibers, fiber birefringence is significantly increased up to approximately 0.19–0.20. This procedure, i.e., unperturbed spinning and posttreatment, is similar to a traditional spin–draw process. On the other hand, the LIB as-spun fibers have high birefringence of 0.17–0.21. The extensibility of the perturbed as-spun fibers is relatively low compared to that of unperturbed fibers. The near maximum draw ratios are 1.2 for 3500 m/min and only 1.1 for 5000 m/min take up as-spun fibers. Although the perturbed fibers were drawn at low draw ratios, the posttreated LIB fibers exhibit ultrahigh birefringence of approximately 0.22–0.23, values which are not obtainable from the traditional process, even though relatively high draw ratio are commonly employed. These values have reached or are actually a little higher than the intrinsic crystalline birefringence of 0.22, as documented by Dumbleton.[15] In the LIB spinning process, the LIB as-spun fibers exhibit high orientation because of the effect of the threadline modifications in both stress and temperature profiles via the liquid bath. These modifications alter the threadline dynamics first and, in turn, the macromolecular chain extension along the fiber axis. Thus, the morphology and mechanical properties are significantly improved.

Tenacity and initial modulus of as-spun fibers of both LIB and unperturbed spinning processes and their respective posttreated fibers are shown in Figures 3 and 4. In general, both tenacity and initial modulus are respective functions of take-up velocity. Tenacity and initial modulus of the posttreated fibers both increased relative to their respective as-spun fibers. Although the unperturbed spun fibers were subjected to drawing and annealing, the posttreated unperturbed (unperturbed/DA) fibers still show lower tenacity than those of the one-step obtained LIB as-spun fibers at take-up speeds of 3000–5000 m/min. At a certain LIB depth of 30 and 45 cm, it is found that the higher the take-up speed, the higher the tenacity. At take-up speeds of 2000–4000 m/min, a LIB depth of 45 cm was used. However, at take-up velocity above 4000 m/min, LIB depth could not be maintained at the same level of 45 cm due to high spinline stress and resulted in frequent breakage in the threadline. Thus, a depth of 30 cm was used at take-up speeds of 4000–5000 m/min. The highest tenacity, 9.6 g/d, of the LIB as-spun fibers was obtained at take-up speed of 5000 m/min. After posttreatment at draw ratio of 1.1, tenacity increased to 10.3 g/d. The highest initial modulus of 147.5 g/d was obtained from posttreated LIB fibers, which was taken up at an intermediate speed of 3500 m/min with a draw ratio of 1.2, as shown in Table I.

Elongation at break of the LIB fibers (see Table I) is 14.8% at 3500 m/min and falls to 10.5% at 5000 m/min. The general finding is, the higher the take-up velocity, the lower the elongation at break. The posttreated LIB fibers have low elongation at break, in the range of approximately 8–11%, while the posttreated unperturbed is 16% or higher. The unperturbed as-spun fibers have crystallinity (X_v) from 7.8 to 39.3% as take-up velocity increased from 2000 to 5000 m/min, as shown in Figure 5. Notice that the crystallinity of the LIB as-spun fibers is gradually suppressed from 2000 to 5000 m/min speed. At 4000 m/min and above, the crystallinity is less than that of unperturbed fibers. In traditional high-speed

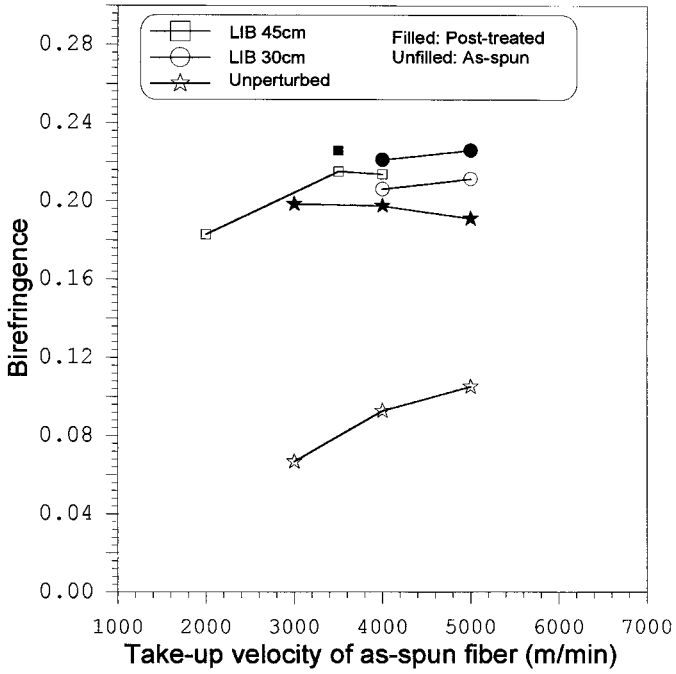

Figure 2 The effect of take-up velocity on birefringence of as-spun and posttreated fibers made by liquid isothermal bath (LIB) spinning process and by unperturbed spinning process under different conditions.

spinning, a fiber with low crystallinity, all other things equal, generally has a higher extensibility than that of fiber with a high crystallinity. In the case of unperturbed fibers, the near maximum draw ratios are 1.7 and 1.5 for the fiber spun at 3000 and 5000 m/min, respectively. However, in

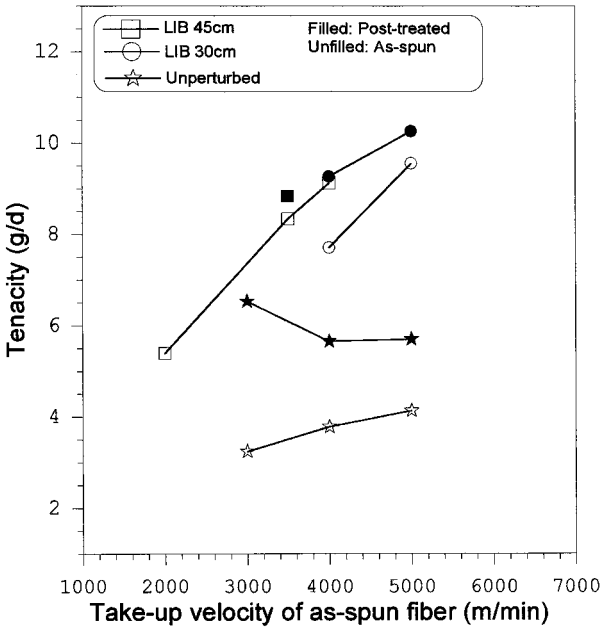

Figure 3 The effect of take-up velocity on tenacity of as-spun and posttreated fibers made by liquid isothermal bath (LIB) spinning process and by unperturbed spinning process under different conditions.

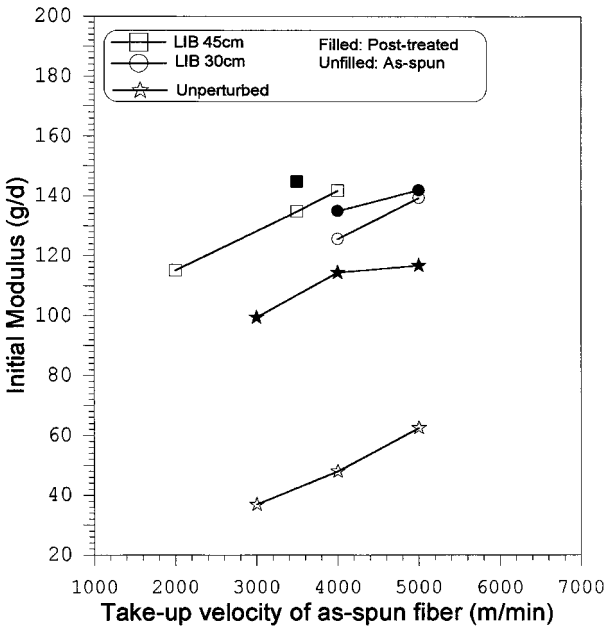

Figure 4 The effect of take-up velocity on initial modulus of as-spun and posttreated fibers made by liquid isothermal bath (LIB) spinning process and unperturbed spinning process under different conditions.

Table I A Comparison of the Mechanical Properties of Liquid Isothermal Bath (LIB) As-Spun and Their Respective Posttreated Fibers with Fibers Made by the Unperturbed Processes Under Different Conditions and With Two Commercial Tire Cords

Take-Up Speed and Process (m/min)	Draw Ratio (DR)	Temperature of 1st Heater (°C)	Temperature of 2nd Heater (°C)	$T : E : M$ (g/d : % : g/d)	LASE-5 (g/d)
3500 LIB[a]	—	N/A	N/A	8.3 : 14.8 : 128.8	3.64
3500 LIB/DA	DR = 1.1	180	N/A	9.1 : 9.7 : 134.1	5.03
3500 LIB/DA	DR = 1.1	180	220	9.1 : 10.7 : 138.9	5.49
3500 LIB/DA	DR = 1.2	180	220	10.0 : 9.8 : 147.5	5.78
5000 LIB[b]	—	N/A	N/A	9.6 : 10.5 : 139.4	5.07
5000 LIB/DA	DR = 1.1	180	220	10.3 : 8.7 : 140.9	5.48
5000 unperturbed[c]	—	N/A	N/A	4.1 : 67.5 : 62.5	1.23
5000 unperturbed/DA	DR = 1.5	180	220	5.7 : 16.1 : 116.8	3.13
Conventional tire cord[d]	Unknown	—	—	9.5 : 16.6 : 96.1	2.94
Low shrinkage tire cord[d]	Unknown	—	—	7.4 : 16.5 : 87.9	3.31

[a] LIB depth = 45 cm; spinning/denier = 6 dpf.
[b] LIB depth = 30 cm; spinning/denier = 4.5 dpb.
[c] Spinning/denier = 4.5 dpf.
[d] From Hotter.[19]
NA = not applicable.

the case of LIB fibers, the near maximum draw ratio is only 1.1–1.3 (see Table III). Although the LIB as-spun fibers have a low crystallinity of 29.1% at the 5000 m/min speed, the draw ratio is still lower than that of the unperturbed fiber made at the same speed, with a high crystallinity of 39.3%. Thus, it appears that the extensibility is not correlated simply to crystallinity (X_v). In the literature, a third phase, or so-called intermediate phase, or oriented mesophase, or oriented amorphous phase, or taut–tie molecular phase, has been discussed by many researchers.[16,20–24] The above-mentioned unique combination of properties, i.e., low crystallinity, low elongation, and high birefringence, might be looked upon as first evidence that the noncrystalline chains of the LIB as-spun fibers are highly ordered or oriented. In addition, with low extensibility (i.e., low draw ratio) exhibited during posttreatment and, at the same time, showing low crystallinity and high birefringence, a second bit of evidence presents itself strengthening the notion that LIB fibers have taut–tie noncrystalline chains in the as-spun stage and in their respective posttreated fibers. These two pieces of evidence, if not proof, at least suggest the presence or existence of a taut–tie noncrystalline phase, referred to as a third phase, in addition to the two phases, i.e., random amorphous and crystalline phases, commonly accepted as existing in the traditional two-phase model.

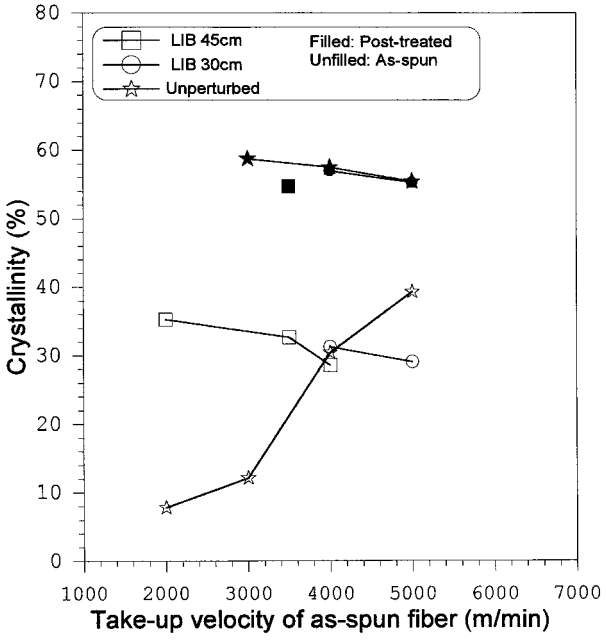

Figure 5 The effect of take-up velocity on crystallinity of as-spun and posttreated fibers made by liquid isothermal bath (LIB) spinning process and by unperturbed spinning process under various conditions.

Further, (see Figure 6 and Table IV) boil-off shrinkage (BOS) of unperturbed as-spun fibers starts high, above 60%, at 2000 m/min and drops off rapidly to approximately 2% at 5000 m/min; while crystallinity increases rapidly and, significantly, from approximately 8 to 39% over the same wind-up speed range. This follows expected behavior. In traditional high-speed spinning, Vas-

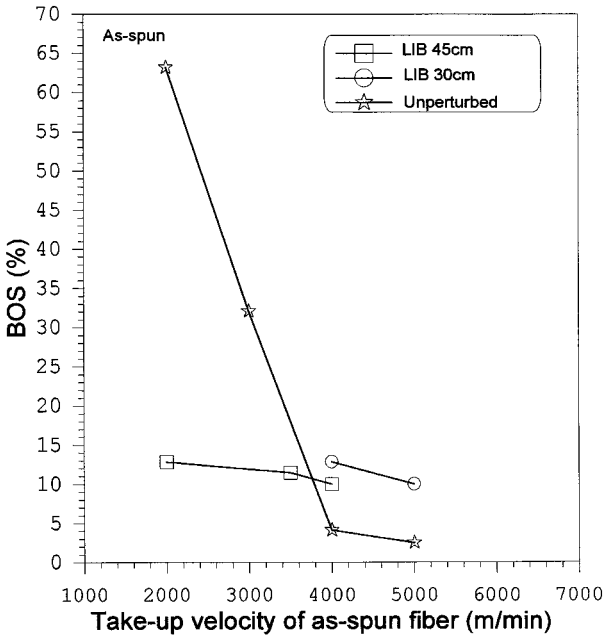

Figure 6 The effect of take-up velocity on boil-off shrinkage (BOS) of as-spun fibers made by liquid isothermal bath (LIB) spinning process and by unperturbed spinning process under various conditions. (Note that the BOS of the unperturbed fibers is based on a repeated experiment.[26])

silatos et al.[27] showed that crystallinity (density related) increases with increasing take-up speed, while BOS decreases. Heuvel and Huisman[28] demonstrated similar dependency of BOS on crystallinity. As is obvious in Figure 6 and Table IV the unperturbed as-spun fibers follow trends presented by Vassilatos et al. and Heuvel and Huisman. On the other hand, as shown in the same figure and table, the BOS of LIB as-spun fibers drops from approximately 13 to 10%, over the same wind-up speed range of 2000 to 5000 m/min, as crystallinity also drops, from 35.3 to 29.1%. The reason for this drop in crystallinity with increasing wind-up speed for LIB fibers has been discussed in a previous publication.[4] The BOS–crystallinity behavior represents a surprising and unique departure from conventional behavior. This suggests that BOS of LIB fibers is not simply dependent upon crystallinity as is the BOS of traditionally high-speed spun fibers. We temporarily delay our proffered rationalization pending publication of an article on "Heat Shrinkage of LIB Fibers," which will relate shrinkage behavior to an altered morphological structure. Notice in Figure 6 and Table IV that the BOS of LIB as-spun fibers is somewhat higher than that of unperturbed fibers produced at 4000 m/min and beyond. This may be related to the lower crystallinity of the LIB fibers formed in this wind-up speed range. Associated with this matter, some interesting/data should be pointed out. While posttreatment, drawing, and/or annealing has been shown to readily overcome this higher thermal shrinkage encountered in some of the as-spun LIB fibers, this solution was unacceptable in our viewpoint because our intent was to produce high-speed spun high performance PET fibers in a one-step process. With this in mind, it is instructive to consider Figure 9, which shows the beneficial effect of increasing bath depth on the properties of tenacity and modulus. This encouraging lead, based on the relationship between depth of liquid in the isothermal bath and tensile properties, will be discussed later as a means of further improving the properties LIB as-spun fibers.

When LIB as-spun fiber was subjected to a continuous two-step posttreatment, as described earlier, essentially, all the drawing occurred in the first step and the annealing occurred in the second. A comparison of the fiber properties of the LIB as-spun and posttreated fibers and the two commercial tire cord fibers is listed in Table I. It is well known that temperature, time, and tension are the three main parameters that control fiber structure development during the spinning, drawing, and annealing processes[29] and that the structure will ultimately determine the final fiber properties. As shown in Table I (3500 m/min), the beneficial effects of posttreatment are certainly evident.

It is obvious that the posttreated LIB fibers have not only higher initial modulus and higher strength, but also higher LASE-5, than either of the two commercial tire cords. The posttreated LIB fibers have LASE-5 of 5.03–5.78 g/d, while the two commercial tire cords have 2.94 and 3.31 g/d, respectively. In addition to superior LASE-5, the posttreated LIB fibers show superior lower thermal shrinkage, at approximately 5%, than any of the conventional or low shrinkage commercial tire cords, as illustrated in Figure 7. Notice that both LASE-5 and thermal shrinkage are considered the two main parameters of dimensional stability. From the results, the posttreated LIB fibers have indeed excellent dimensional stability, superior to that of the traditional spin–draw fibers and the two commercial tire cord fibers.

The Effect of Liquid Isothermal Bath Depth Under Conditions of High-Speed Spinning

Figure 8 shows typical stress–strain curves of as-spun and posttreated fibers of both LIB and un-

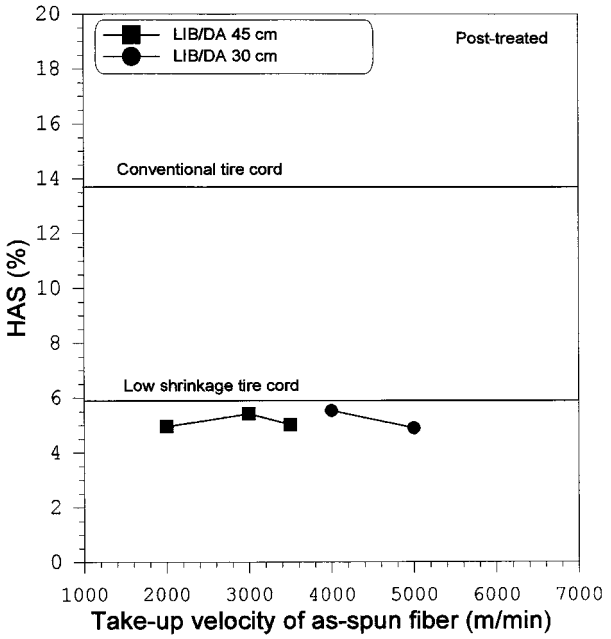

Figure 7 A comparison of hot air shrinkage (HAS) between commercial tire cord and the posttreated LIB fibers at different take-up velocities and liquid depths.

perturbed fibers produced at 5000 m/min take-up speed. Typical stress–strain curves of the conventional and the low shrinkage commercial tire cord fibers are also included for comparison. In the case of unperturbed as-spun fibers, low strength low modulus and very high elongation at break, above 80%, are the accepted norm.[1] After posttreatment of the unperturbed fibers, tenacity and initial modulus increase to approximately 6 and 117 g/d, respectively; and elongation at break drops to approximately 16%. The low shrinkage tire cord has lower strength than that of conventional tire cord but has better dimensional stability than that of conventional fiber, as seen in Table I and Figure 7. Notice that the two commercial tire cord fibers have essentially the same elongation at break of approximately 16%. Although the two commercial tire cords and the unperturbed fibers have been drawn to their near-maximum draw ratio, elongation at break of these fibers is still higher than that of posttreated LIB fibers. The posttreated LIB fiber has low elongation at break, less than 10%, and is not obtainable by the conventional unperturbed spin–draw process. At 5000 m/min, the LIB as-spun fiber has not only slightly higher strength but also higher initial modulus than either of the commercial tire cord fibers. The posttreated LIB fibers have even higher strength, higher initial modulus, higher LASE-5, and lower thermal shrinkage than those of their respective as-spun fibers. This combination of superior mechanical properties and excellent dimensional stability is never obtained from any of the two commercial tire cord fibers. The effect of the stress-enhanced LIB spinning on structural parameters is discussed in the next section.

Figures 9 and 10 show the respective effect of LIB depth on mechanical properties, LASE-5, and thermal shrinkage of both LIB as-spun and posttreated fibers. The LIB depth was increased from 20 to 30 cm. As stated in the previous publication,[4] the greater the liquid level, the higher the spinline stress. This situation produces higher birefringence in the as-spun fibers than is found in the unperturbed fibers. The difference in tenacity between as-spun and posttreated fibers is 2.4 g/d, from 7.1 to 9.5 g/d, at LIB depth of 20 cm. At a higher LIB depth of 30 cm, the difference is only 0.7 g/d, from 9.6 to 10.3 g/d. The same tendency is also shown in initial modulus. The difference is 21.7 g/d, from 117.2 to 138.9 g/d, at LIB depth of 20 cm; while it is only 1.5 g/d, from 139.4 to 140.9 g/d, at LIB depth of 30 cm. LASE-5, in Figure 10, also shows the same trend. The difference in LASE-5 between as-spun and posttreated fibers is 1.11 g/d, from 4.26 to 5.37 g/d, at LIB depth of

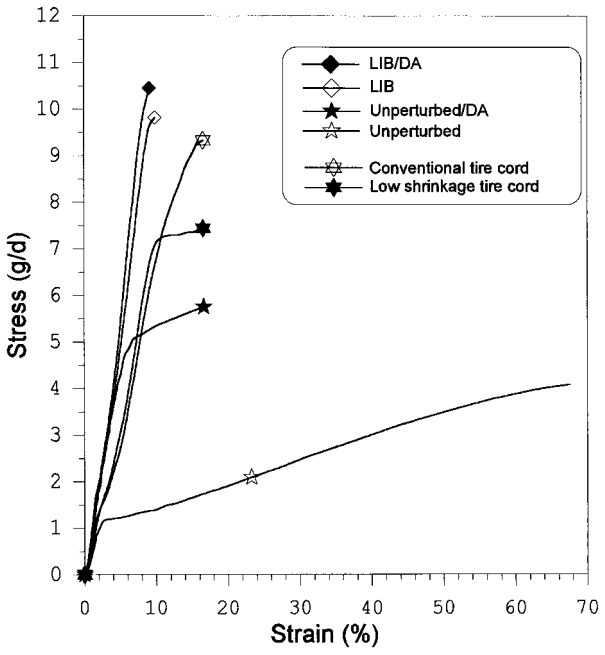

Figure 8 Typical stress–strain curves of as-spun (5000 m/min take-up) and the respective posttreated fibers made by liquid isothermal bath (LIB) spinning process and by unperturbed spinning process, compared with stress–strain curves of commercial tire cord fibers.

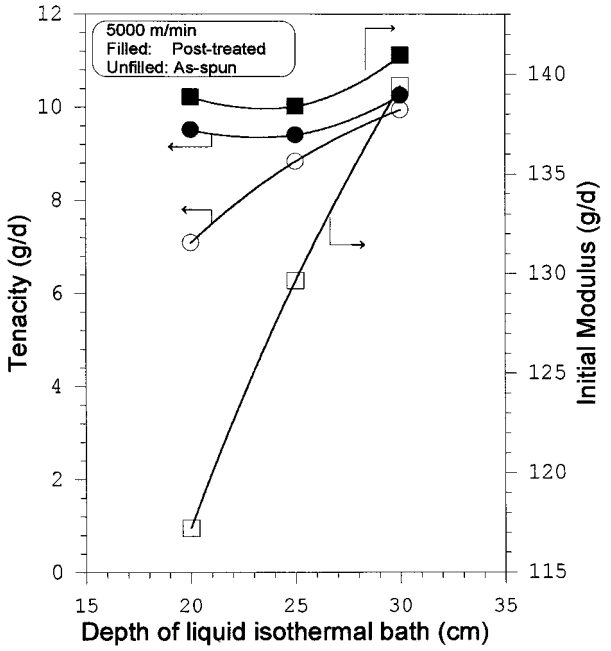

Figure 9 The effect of LIB depth at take-up velocity of 5000 m/min on fiber tenacity and initial modulus of as-spun and the respective posttreated fibers.

20 cm; while it is only 0.41 g/d, from 5.07 to 5.48 g/d, at LIB depth of 30 cm. According to the results, as LIB depth was increased from 20 to 30 cm, the properties of the as-spun fibers are closer to those of their respective posttreated fibers. This is an important and suggestive finding. It lends credence to the statement that the LIB spinning process has the potential to produce high-performance fiber via high-speed spinning in one step instead of the traditional two steps. Work is continuing on this matter.

At 5000 m/min (see Table V), the volume crystallinity of LIB as-spun fibers decreased from approximately 32 to 29% when the LIB depth increased from 20 to 30 cm. As the threadline stress was increased by introduction of the liquid isothermal bath, crystal growth was suppressed and resulted in a reduction of crystallinity.[3] In general, the effect of the increasing LIB depth on crystallinity reduction is similar to the effect of the increasing take-up velocity on crystallinity, as described above. Since molecular chains are stretched under high tension and the fiber exhibits its low crystallinity, the fraction of taut–tie molecular chains should be increased. Although all the posttreated LIB fibers have essentially the same crystallinity (X_v) of approximately 55%, the thermal shrinkage of the fibers still is a weak function of LIB depth. The higher the LIB depth, the lower the thermal shrinkage found (see Figure 10). The thermal shrinkage of the posttreated fibers seem to show a dependence on the spinline stress that they experienced during their passage through the liquid isothermal bath, where the oriented macromolecular structure was developed.

Structure of As-Spun and Posttreated Fibers

In the LIB spinning process, both stress and temperature profiles were modified via controlled threadline dynamics.[2] Unlike unperturbed fibers, the discussed unique properties of low crystallinity and high birefringence imply that the occurrence of folded chains has been reduced, and that of extended chains has increased. Moreover, with the properties of high birefringence, low crystallinity, and the propensity of low draw ratio, the existence of taut–tie molecular chains in the noncrystalline region seems reasonable and acceptable. Orientational nucleation then proceeds rapidly to induce orientational crystallinity during postdrawing and annealing. Meanwhile, taut–tie molecular chains are further developed and crystallized.

Radial birefringence of as-spun and posttreated fibers is shown in Figure 11. After posttreatment, birefringence of both the LIB and unperturbed fibers has increased when compared to

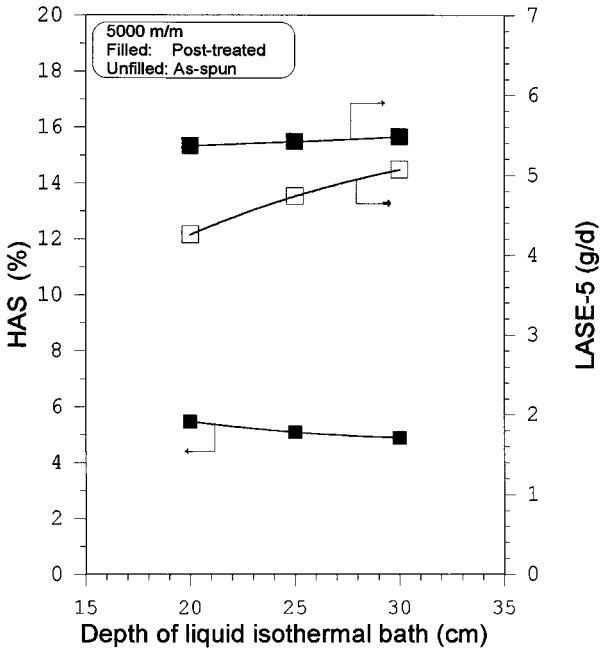

Figure 10 The effect of LIB depth at take-up velocity of 5000 m/min on hot air shrinkage (HAS) and load at a specified elongation of 5% (LASE-5) of as-spun and their respective posttreated fibers.

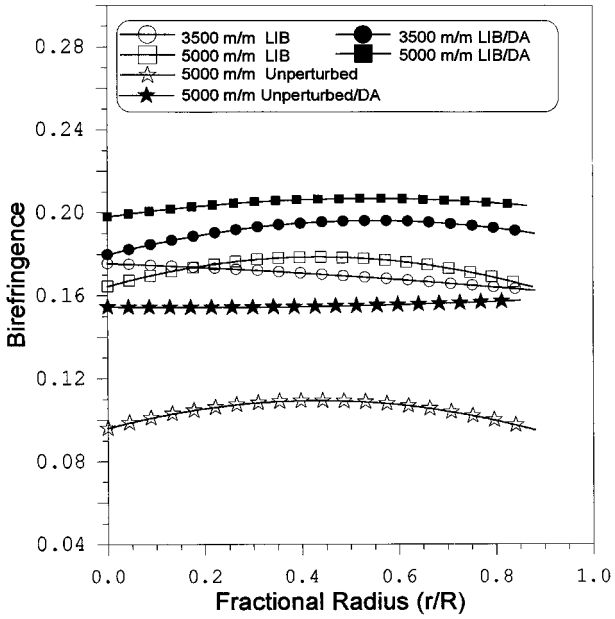

Figure 11 Radial distribution of birefringence of as-spun and the respective posttreated fibers made by liquid isothermal bath (LIB) spinning process and by unperturbed spinning process.

their respective as-spun fibers. In general, the as-spun and the posttreated fibers are essentially radially uniform, as shown in Figure 11. This is an important point. We feel that any closer approach of properties to the calculable, high theoretical levels can be made only if a uniform radial structure can be produced.

Crystallization during spinning of the unperturbed as-spun fibers proceeds following the concepts of stress-induced crystallization.[30] As shown in Figure 5, the crystallinity (X_v) is increased from 7.8 to 39.3% when take-up speed is increased from 2000 to 5000 m/min. In the case of the perturbed fibers spun at low speeds of 2000–3500 m/min with LIB temperature of 175°C, crystallinity (ca. 35%) is higher than that of unperturbed fiber at each take-up speed. These results show the significant effect of the temperature modification of the LIB spinning system on fiber crystallinity. The increased crystallinity of the LIB as-spun fiber is due to the low spinline stress (at low take-up speed), the high liquid temperature of 175°C, and the long/depth of 45 cm, giving a longer resident time when the fiber passes through the liquid isotherm bath. However, when the take-up speed is increased to 4000 m/min and above, spinline stress is increased; and crystallinity of the LIB spun fibers is significantly suppressed when the unperturbed fibers are compared at each take-up speed. At 5000 m/min (see Fig. 5), the crystallization of the unperturbed fiber is 39.3%, while that of the LIB fiber is only 29.1%. In Table II, it is clear that crystal growth of the LIB as-spun fiber is significantly suppressed when apparent crystal size at the reflection planes of (010), (100), and ($\bar{1}$05) is compared with that of unperturbed fiber. This effect has been reported earlier in our work.[4]

After posttreatment, the apparent crystal sizes of L_{010}, L_{100}, and $L_{\bar{1}05}$ of the LIB posttreated fibers are still smaller than those of posttreated unperturbed fiber. The posttreated LIB and unperturbed fibers have essentially the same crystallinity (X_v) of approximately 55%, as shown in Table III. The same crystallinity level and the small crystal dimensions imply that the number of crystals in the posttreated LIB fiber is greater than that of posttreated unperturbed fiber. This means that the distance between crystals is shortened, i.e., shorter noncrystalline chains are formed. In addition, the unique high amorphous orientation factor (f_a) of approximately 0.85–0.90 (see Table III) is higher than that of unperturbed fiber f_a of below 0.70. It implies that the noncrystalline

Table II Apparent Crystal Size, Crystalline Orientation Factor (f_c) and Amorphous Orientation Factor (f_a) of As-Spun Fibers Spun by Liquid Isothermal Bath (LIB) and Unperturbed Spinning Processes

Take-Up Speed and Spinning Process (m/min)	Apparent Crystal Size (Å)				
	L_{010}	L_{100}	$L_{\bar{1}05}$	f_c	f_a
2000 LIB[a]	41.5	30.7	48.2	0.886	0.585
3500 LIB[a]	40.9	31.3	47.2	0.862	0.757
5000 LIB[b]	36.8	33.7	45.4	0.922	0.795
3000 unperturbed	16.6	20.3	36.6	0.854	0.138
5000 unperturbed	44.0	42.5	54.4	0.916	0.153

[a] LIB depth = 45cm; spinning/denier = 6dpf.
[b] LIB depth = 30cm, spinning/denier = 4.5dpf.

Table III Draw Ratio (DR), Crystallinity (X_v) Apparent Crystal Size, Crystalline Orientation Factor (f_c) and Amorphous Orientation Factor (f_a) of Posttreated LIB and Unperturbed Fibers and Commercial Tire Cord

Take-Up Speed & Spin-Draw Process (m/min)	Draw Ratio (DR)	X_v (%)	Apparent Crystal Size (Å)			f_c	f_a
			L_{010}	L_{100}	$L_{\bar{1}05}$		
2000 LIB/DA	1.3	53.4	57.5	43.3	62.1	0.945	0.848
3500 LIB/DA	1.2	55.3	58.6	41.4	60.0	0.956	0.896
5000 LIB/DA	1.1	55.3	52.5	41.6	58.0	0.946	0.901
Low shrinkage tire cord	Unknown	45.3	49.8	37.4	54.9	0.936	0.723
3000 unperturbed/DA	1.7	58.8	63.2	43.1	59.0	0.940	0.679
5000 unperturbed/DA	1.5	55.4	76.5	54.2	58.9	0.926	0.641

chains are highly extended. The high amorphous orientation factor (f_a) from X-ray analysis agrees with the high birefringence obtained from the polarizing microscope measurement and strongly supports the assumption that the noncrystalline region makes a dominating contribution toward the high orientation detected. This provides the third piece of evidence for the likely existence of a taut–tie noncrystalline phase in the LIB as-spun and posttreated fibers.

The relationship between tenacity and f_a has been reported by Samuels[31] and Rim and Nelson.[7] In LIB fibers, it is believed that the presence of the unique combination of short taut–tie molecules and the high f_a should result in significantly improving both tenacity and initial modulus.

Figure 12 presents DSC curves of as-spun and their respective posttreated LIB fibers made at a low-speed spinning of 2000 m/min and an intermediate-speed of 3500 m/min. The unperturbed as-spun (2000 m/min) and posttreated fibers are used as controls and are also shown for comparison. In the case of unperturbed 2000 m/min speed as-spun fiber, a T_g is observed. The T_g occurrence is common and is observed for fibers spun at take-up speeds below 5000 m/min.[20,28] However, it is not observed in the LIB as-spun fibers at the same take-up speed. This may be because the LIB as-spun fiber has relatively high crystallinity of approximately 35.3%, as discussed above, while the crystallinity of the unperturbed fiber is only approximately 7.8%. At 5000 m/min, unlike the LIB as-spun fibers, the unperturbed as-spun fiber has a broad melting range, i.e., from initial melting to final melting, as shown in Figure 13. The broad melting range indicates the unperturbed as-spun fiber possesses less uniform structure than does LIB as-spun fiber, which shows a narrow melting range.

It has been documented that DSC curves do not represent the state of the fiber at room temperature before the DSC scan.[32] During DSC scanning, the polymer is subjected to a perfection process with competition between partial melting

Table IV Boil-Off Shrinkage (BOS) and Crystallinity (X_v) of As-Spun Fibers Made by Unperturbed Spinning Process Shown in the Original Data[25] (A) and Repeat Experiments[26] (B) and by LIB Spinning Process Shown in the Original Data[25] (A)

Take-up Speed (m/min)	Unperturbed				LIB	
	BOS (%)		X_v (%)		BOS (%)	X_v (%)
	A	B	A	B	A	A
2000	—	63.2	—	7.8	12.9[b]	35.3[b]
3000	7.1[a]	32.1	19.1	12.1	—	—
4000	3.6	4.1	31.7	30.4	10.0[b], 12.9[c]	28.6[b], 31.3[c]
5000	2.9	2.5	39.5	39.3	10.0[c]	29.1[c]

[a] Based upon many replicate measurements by several researchers, this value was considered incorrect and was rejected.
[b] LIB, 45cm.
[c] LIB, 30cm.

Table V The Effect of LIB Depth on Individual Fraction of Taut–Tie Noncrystalline Phase (TTNC %), Initial Modulus, and Crystallinity (X_v) of the LIB As-Spun Fibers Spun at Take-Up Speed of 5000 m/min

LIB Depth (cm)	Fraction of Taut–Tie Noncrystalline Phase (%)	Initial Modulus (g/d)	X_v (%)
20	10.69	117.2	32.3
25	12.21	129.7	27.7
30	13.31	139.4	29.1
w/o LIB	4.06	62.5	39.5

Unperturbed (w/o LIB) as-spun fiber are also included for comparison.

and recrystallization before the polymer is totally melted.[32] The phenomenon of two endothermic peaks of PET polymer are the result of initial melting, immediately followed by recrystallization, and has been discussed by many researchers.[32–34] For the experimental LIB as-spun fiber take-up at 2000 m/min with LIB depth of 45 cm (see Fig. 12), the first melting peak, i.e., the lower melting peak, is broad and undefined. At the same LIB depth, the first melting peak becomes clear and sharp when the take-up is increased to 3500 m/min. Further (see Fig. 13), the first melting peak of the LIB fibers spun at 5000 m/min speed changed gradually from an unresolved peak to a resolved sharp peak when the LIB depth is increased from 20 to 30 cm. Notice that either an increase in take-up speed or an increase of LIB depth results in the same effect of increasing threadline stress. As previously reported,[4] the increased threadline stress via the introduction of the LIB on the threadline is beneficial in developing extended macromolecular chains. Table V shows that the fraction of the taut–tie noncrystalline phase is proportional to the LIB depth. This indicates that the first melting peak may be intimately related to the developing structure of extended macromolecular chains.

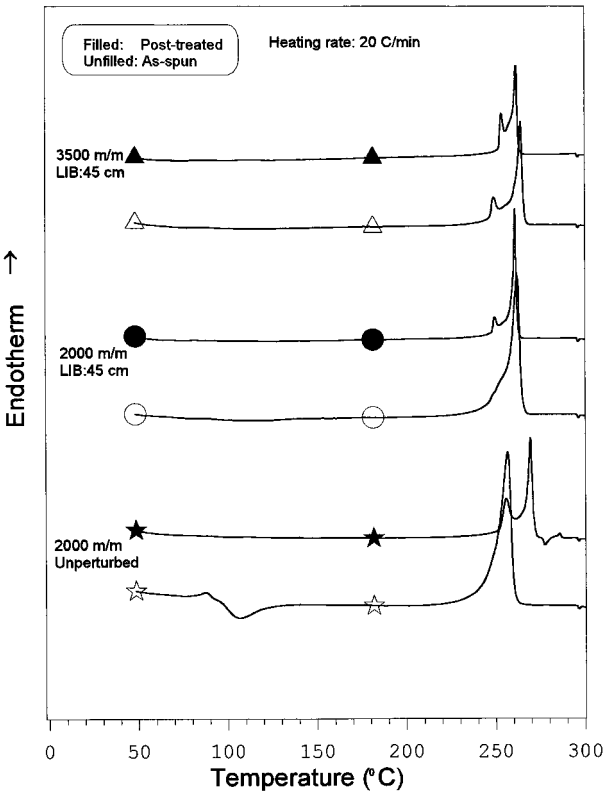

Figure 12 DSC curves of as-spun and their respective posttreated liquid isothermal bath (LIB) fibers and unperturbed fibers under various conditions.

Further, after posttreatment of the LIB fibers, the first melting peak not only becomes sharper but is also shifted to slightly higher temperature. This melting behavior is similar to that reported by Peterlin and Meinel for polyethylene.[35] Shifting of the first melting peak to higher temperature may be related to the increase of the apparent crystal sizes of L_{010}, L_{100}, and $L_{\bar{1}05}$ in the posttreated fibers, as seen by comparing values in Tables II and III. Peterlin and Meinel[35] suggested that the narrowing of the melting peak, and the shift of the peak to higher temperature might be due to the presence of many taut–tie molecules, which delay partial melting. In this report, the posttreated LIB fibers demonstrate a higher fraction of taut–tie noncrystalline phase (TTNC %) than their respective as-spun fibers. This is discussed in the next section. Moreover, the temperature difference between the two melting peaks is decreased in the posttreated fibers. The results illustrate that the posttreated fibers have a faster recrystallization rate than those of their respective as-spun fibers during the DSC scan. These results agree with the explanation by Smith and Steward.[36]

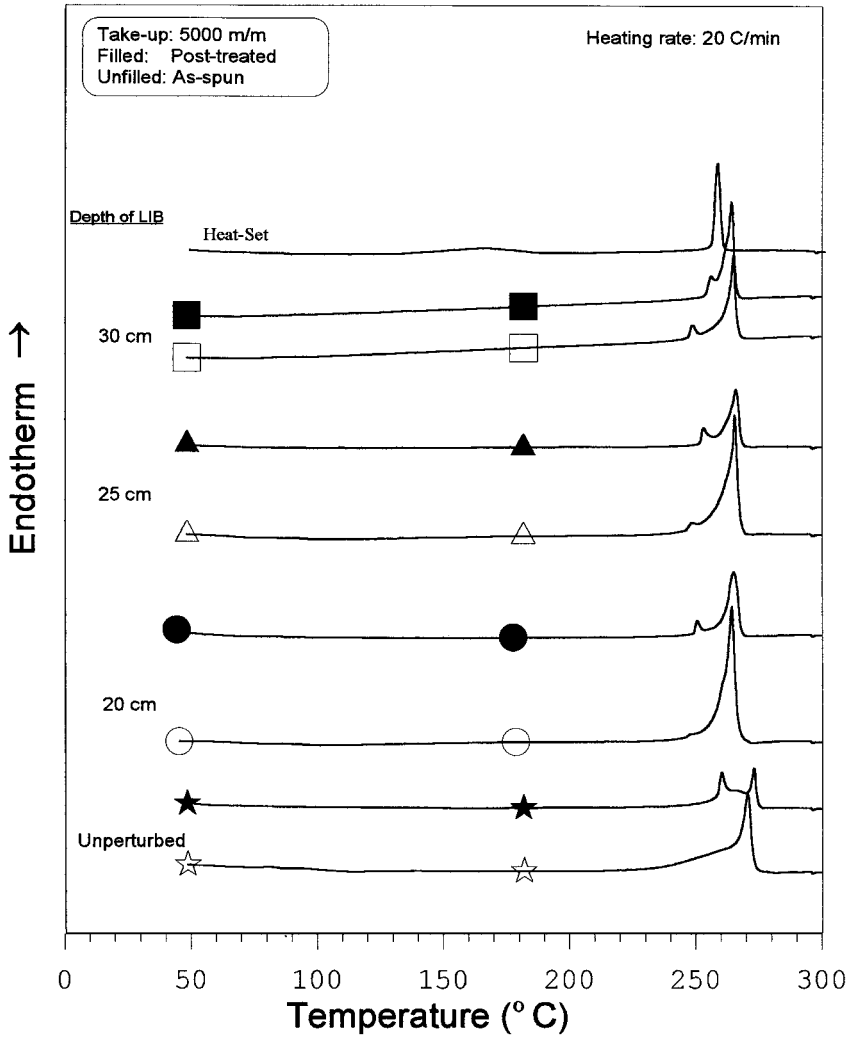

Figure 13 DSC curves of as-spun and their respective posttreated fibers at constant take-up velocity of 5000 m/min made by liquid isothermal bath (LIB) spinning process and by unperturbed spinning process at various liquid depths.

With additional heat-setting of the posttreated fiber (LIB depth = 30 cm; 5000 m/min take-up) at 180°C for 10 min at constant length, the DSC curve becomes a single narrow melting peak, as shown in the top curve of Figure 13. The single narrow melting peak, located between the two endothermic peaks of the respective as-spun or posttreated fibers, suggests that the heat-set fiber has a larger and more uniform crystal structure. Concerning the two endothermic peaks, Bell and Murayama[37] documented that the area of the low-temperature peak increased; whereas the area of the high-temperature peak decreased as exposure time to thermal treatment increased. Further, the low-temperature peak tended to shift to higher temperature as annealing time increased. Our results agree generally with those of Bell and Murayama.[36] This behavior suggests that the single narrow melting peak (see Fig. 13) might be derived from the first melting peak of both the as-spun and posttreated fibers, respectively. With regard to the purported unique extended chain structure of LIB as-spun and posttreated fibers, further detailed thermal analysis is underway.

The Relationships Among Structural Properties

Figure 14 shows that the fiber tenacity and initial modulus of the posttreated LIB fibers is dependent upon the birefringence of their as-spun fibers. In the case of the unperturbed fibers, the high-speed spun fiber (5000 m/min) with the highest birefringence of 0.105 continues the upward pattern of initial modulus of the respective

posttreated fibers with increasing birefringence; while the tenacity of the posttreated fiber drops, at the same birefringence. This is one more manifestation seen scattered in the literature and in our own results, indicating that the general acceptance of the concept that initial modulus and tenacity are both closely related to birefringence. The details of these respective relations or dependencies are different and still obscure.

Both crystalline and noncrystalline parts contribute to orientation. Table III illustrates that crystalline orientation factor (f_c) of all the posttreated fibers have reached approximately 0.92 to 0.96. The amorphous orientation factor (f_a) of the posttreated LIB fibers is approximately 0.85 or higher, while it is relatively low at approximately 0.72 or less in the low shrinkage tire cord and the posttreated unperturbed fibers. It seems that the overall orientation is dominated by the noncrystalline contribution.

The fraction of taut–tie noncrystalline phase (TTNC %) is calculated on the basis of a parallel-series three-phase model proposed by Kamezawa et al.[17] In the as-spun fibers, the fraction of taut–tie noncrystalline phase of the LIB fibers is significantly higher than that of unperturbed fibers, as shown in Table V. When the LIB depth increased from 20 to 30 cm at a take-up speed of 5000 m/min, the fraction of the taut–tie noncrystalline phase is proportionally increased. As shown in Figure 15, a linear relationship is found between the fraction of the taut–tie noncrystalline phase and initial modulus of PET fibers.

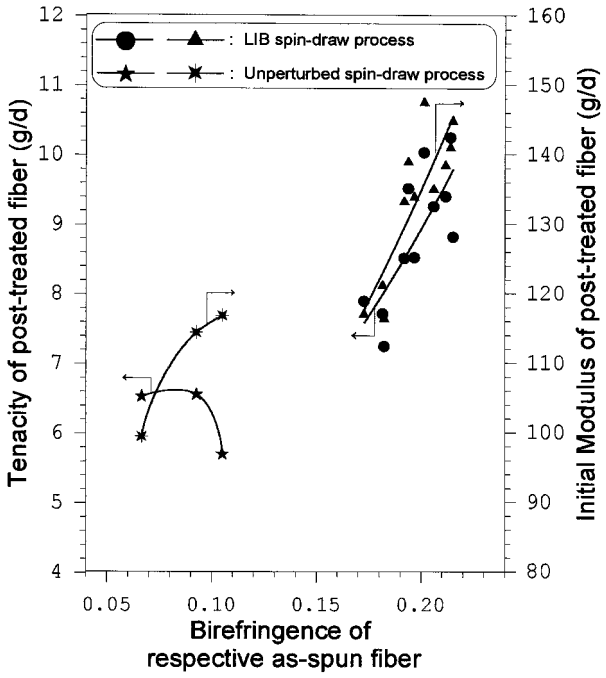

Figure 14 Fiber tenacity and initial modulus of posttreated liquid isothermal bath (LIB) fibers and unperturbed fibers versus birefringence of their respective as-spun fibers.

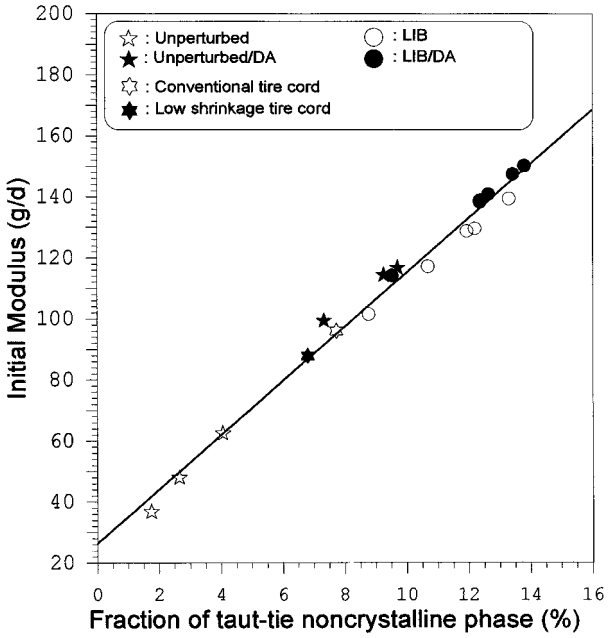

Figure 15 The relationship between initial modulus and the fraction of taut–tie noncrystalline phase (TTNC %) of PET fibers obtained from different processes indicated in the inset.

CONCLUSIONS

Fibers made by controlled threadline dynamics via liquid isotherm bath (LIB) spinning and subsequent posttreatment at low draw ratios demonstrate superior mechanical properties and excellent dimensional stability. They also exhibit unique characteristics possessing high amorphous orientation, high fraction of taut–tie noncrystalline phase with low crystallinity, and exhibit high strength and high initial modulus in the as-spun state. The high fraction of taut–tie noncrystalline phase is produced by the stress-enhanced LIB spinning system. Further, with postdrawing and annealing, the extended chains of LIB as-spun fibers are further rapidly developed and crystallized along the fiber axis. In addition, the enhanced fraction of taut–tie noncrystalline chains with shorter length play a dominant role in the structure responsible for the unique combination of superior properties. The mechanical properties of the posttreated LIB fibers exhibit

a strong/dependency on the birefringence of their respective as-spun fibers. Moreover, it is found that overall orientation is dominated by the noncrystalline contribution. The calculated fraction of the taut–tie noncrystalline phase agrees with and strongly supports evidence for the existence of a third phase in addition to those generally accepted in the traditional two-phase model. It is also speculated that initial modulus is primarily determined by the fraction of the taut–tie noncrystalline phase present in the PET fibers. The LIB-draw process demonstrates the capability of producing high-performance fibers with a combination of properties not obtainable by traditional processes used to produce commercial and even "experimental" tire cord.

The authors wish to express their appreciation for financial support from AlliedSignal and Hoechst Celanese. We give special thanks to Drs. G. Wu and B. Huang for their many useful discussions and Mr. F. Lundberg for his helpful assistance in sample preparation.

REFERENCES

1. T. Kawaguchi, in *High-Speed Fiber Spinning,* A. Ziabicki and H. Kawai, Eds., Wiley-Interscience, New York, 1985, Chap. 1.
2. J. A. Cuculo, P. A. Tucker, and G. Y. Chen, *J. Appl. Polym. Sci., Appl. Polym. Symp.,* **47,** 223 (1991).
3. C. Y. Lin, P. A. Tucker, and J. A. Cuculo, *J. Appl. Polym. Sci.,* **46,** 531 (1992).
4. G. Wu, Q. Zhou, J. Y. Chen, J. F. Hotter, P. A. Tucker, and J. A. Cuculo, *J. Appl. Polym. Sci.,* **55,** 1275 (1995).
5. Q. Zhou, G. Wu, P. A. Tucker, and J. A. Cuculo, *J. Polym. Sci., Polym. Phys.,* **33,** 909 (1995).
6. G. Wu, P. A. Tucker, and J. A. Cuculo, *Polymer,* **38,** 5, 1091 (1997).
7. P. B. Rim and C. J. Nelson, *J. Appl. Polym. Sci.,* **42,** 1807 (1991).
8. *ASTM D 4974-89,* 1989, ASTM, 1989.
9. L. E. Alexander, *X-Ray Diffraction Methods in Polymer Science,* Krieger, Malabar, 1985, p. 191.
10. C. Y. Lin, J. A. Cuculo, and P. A. Tucker, unpublished Internal Report, 1988.
11. H. M. Heuvel, R. Huisman, and K. C. J. B. Lind, *J. Polym. Sci., Polym. Phys. Ed.,* **14,** 921 (1976).
12. H. M. Heuvel, R. Huisman, *J. Appl. Polym. Sci.,* **22,** 2229 (1978).
13. N. S. Murthy, S. T. Correale, and H. Minor, *Macromolecules,* **24,** 1185 (1991).
14. C. Y. Lin, J. A. Cuculo, and P. A. Tucker, unpublished results, 1988, p. 335.
15. J. H. Dumbleton, *J. Polym. Sci.,* **6,** 795 (1968).
16. M. Kamezawa, K. Yamada, and M. Takayanagi, *J. Appl. Polym. Sci.,* **24,** 1227 (1979).
17. C. L. Choy, M. Ito, and R. S. Porter, *J. Polym. Sci., Polym. Phys.,* **21,** 1427 (1983).
18. T. Thistlethwaite, R. Jakeways, and I. M. Ward, *Polymer,* **29,** 61 (1988).
19. J. F. Hotter, *Commercial Yarn Characterizations Results,* unpublished Internal Report, 1994.
20. J. Shimizu, N. Okui, and K. Kikutani, in *High-Speed Fiber Spinning,* A. Ziabicki and H. Kawai, Eds., Wiley-Interscience, New York, 1985, Chap. 15.
21. A. Peterlin, in *Ultra-High Modulus Polymers,* A. Ciferri and I. M. Ward, Eds., Applied Science, London, 1979, Chap. 10.
22. T. Sun, A. Zhang, F. M. Li, and R. S. Porter, *Polymer,* **29,** 2115 (1988).
23. H. A. Hristor and J. M. Schultz, *J. Polym. Sci., Polym. Phys.,* **28,** 1647 (1990).
24. G. Wu, J.-D. Jiang, P. A. Tucker, and J. A. Cuculo, *J. Polym. Sci., Polym. Phys.,* **34,** 2035 (1996).
25. J. Y. Chen, Ph.D. thesis, North Carolina State University, 1995.
26. G. Wu, P. A. Tucker, and J. A. Cuculo, unpublished internal report.
27. G. Vassilatos, G. H. Knox, and H. R. E. Frankfort, in *High-Speed Fiber Spinning,* A. Ziabicki and H. Kawai, Eds., Wiley-Interscience, New York, 1985, Chap. 14.
28. H. M. Heuvel and R. Huisman, in *High-Speed Fiber Spinning,* A. Ziabicki and H. Kawai, Eds., Wiley-Interscience, New York, 1985, Chap. 11.
29. A. Ziabicki, *Fundamentals of Fiber Formation,* Wiley-Interscience, London, 1976.
30. A. Ziabicki, in *High-Speed Fiber Spinning,* A. Ziabicki and H. Kawai, Eds., Wiley-Interscience, New York, 1985, Chap. 2.
31. R. J. Samuels, *J. Appl. Polym. Sci.,* **10,** 781 (1972).
32. P. J. Holdsworth and A. Turner-Jones, *Polymer,* **12,** 195 (1971).
33. S. Fakirov, E. W. Fischer, R. Hoffmann, and G. F. Schmidt, *Polymer,* **18,** 1121 (1980).
34. B. Wunderlich, *Macromolecular Physics, Crystal Melting,* Vol. 3, Academic, London, 1980.
35. A. Peterlin and G. Meinei, *J. Appl. Polym. Sci., Appl. Polym. Symp.,* **2,** 85 (1966).
36. F. S. Smith and R. D. Steward, *Polymer,* **15,** 283 (1974).
37. J. P. Bell and T. Murayama, *J. Polym. Sci.,* **7,** 1059 (1969).